UCRL-JRNL-223503

LAWRENCE
LIVERMORE
NATIONAL
LABORATORY

GQ Lup Ab Visible & Near-Infrared Photometric Analysis

C. Marois, B. Macintosh, T. Barman

August 8, 2006

The Astrophysical Journal Letters

GQ Lup Ab Visible & Near-Infrared Photometric Analysis

Christian Marois[a], Bruce Macintosh[a], Travis Barman[b]

[a] *Institute of Geophysics and Planetary Physics L-413, Lawrence Livermore National Laboratory, 7000 East Ave, Livermore, CA 94550*

[b] *Lowell Observatory, 1400 W. Mars Hill Rd., Flagstaff, AZ 86001*

ABSTRACT

We have re-analyzed archival HST R and I band images and Subaru CH_4, H, Ks and L′ data of the recently discovered planetary mass companion (PMC) GQ Lup Ab. With these we produce the first R and I band photometry of the companion and fit a radius and effective temperature using detailed model atmospheres. We find an effective temperature of 2338 ± 100K, and a radius of $0.37 \pm 0.05 R_\odot$ and luminosity of $log(L/L_\odot) = -2.43 \pm 0.07$ (at 140pc). Since we fit wavelengths that span most of the emitted radiation from GQ Lup this luminosity estimate is robust, with uncertainty dominated by the distance uncertainty. The radius obtained for 140pc ($0.37 R_\odot$) is significantly larger than the one originally derived. The mass of the object is much more model-dependent than the radiative properties, but for the GAIA dusty models we find a mass between 9-20 $M_{\rm Jup}$, in the range of the brown dwarf and PMC deuterium burning boundary. Assuming a distance of 140pc, observations fit to 1σ the Baraffe evolution model for a ~ 15 $M_{\rm Jup}$ brown dwarf. Additionally, the F606W photometric band is significantly overluminous compared to model predictions. Such overluminosity could be explained by a bright Hα emission from chromospheric activity, interaction with another undetected companion, or accretion. Assuming that GQ Lup Ab has a bright Hα emission line, its Hα emission strength is $10^{-1.71\pm0.10} L_{\rm bol}$, significantly larger than field late-type dwarfs. GQ Lup Ab might be strongly accreting and still be in its formation phase.

Subject headings: stars: imaging, stars: pre-main sequence, stars: low-mass, brown dwarfs, (stars:) planetary systems, techniques: photometric

Suggested running page header: GQ Lup Ab Photometric Analysis

1. Introduction

Direct exoplanet detection around stars is a challenging endeavor, but possible for companions to the youngest stars (Neuhäuser et al. 2005; Chauvin et al. 2005a,b). Unlike the exoplanets found by precision radial velocity techniques, the physical properties of these planetary mass companions (PMCs) must be inferred by comparing atmosphere and evolution models to observed spectra or photometry.

One of the most recent PMC candidates identified orbits the star GQ Lup A (Neuhäuser et al. 2005). This star is a young K7eV TTauri star in the Lupus I cloud (Tachihara et al. 1996). The star has an estimated age of less than 2Myr (Neuhäuser et al. 2005) and is situated at 140pc with a potential range from 90 to 190pc (Wichmann et al. 1998; Neuhäuser & Brandner 1998; Knude & Hog 1998). The original analysis of the GQ Lup A PMC candidate, called GQ Lup Ab, is based on K- and L′-band photometry along with a K-band spectrum. From this early work, an effective temperature of 2050 ± 450K, a radius of $0.12 \pm 0.06 R_{\odot}$, a luminosity of $log(L/L_{\odot}) = -2.37 \pm 0.41$ and log$g$ of 2.5 ± 0.8 are obtained (Neuhäuser et al. 2005; Neuhäuser 2005).

Since other wavelength bands are available from HST and Subaru that span most of the radiation emitted by GQ Lup Ab, it is possible conduct a more complete photometric analysis. This analysis is present below along with the implications of a detected R-band overluminosity.

2. GQ Lup Photometry

In addition to the Neuhäuser et al. (2005) VLT data, GQ Lup Ab has been previously observed by both the Subaru telescope, program o02312, and the Hubble Space Telescope (HST), programs SNAP7387 and 9845. The coronagraphic imager with adaptive optics instrument (CIAO) (Murakawa et al. 2004) was used at the Subaru telescope while the Wide Field Planetary Camera No. 2 (WFPC2) and NICMOS were used with HST.

2.1. HST Visible and NIR Photometry

Data were retrieved from the public MAST Hubble Space Telescope archive at STScI for the filters F606W, F814W, F171M, F190N and F215N using the automated reduction pipeline. The companion is clearly visible 0.7″ west of GQ Lup A in all filters. The GQ Lup A PSF in each filter was first subtracted using reference PSFs of a second star observed in the same program or using simulated PSFs produced by the Tiny Tim software (Krist 1993), selecting the one that gives the smallest residual at $0.7''$ separation. The simulated PSFs in each filter were then used to estimate the GQ Lup Ab flux. PSFs were simulated with five times the sampling, shifted, and binned to the detector resolution. The set of parameters, i.e. fractional pixel PSF position and flux normalization, that minimize the RMS noise inside a 6×6 pixels box centered on GQ Lup Ab was kept. Magnitude errors were estimated by calculating the RMS value of the total GQ Lup A subtracted PSF residual flux at the same angular separation using the same 6×6 pixels box but at a different field angle. Regions contaminated by residual flux from the diffraction spider were avoided. Total companion fluxes were obtained by integrating the Tiny Tim simulated PSFs that best subtract the GQ Lup Ab PSF. The WFPC2 charge-Transfer efficiency bias was corrected (Whitmore et al. 1999), but the amplitude of the effect is small, less than 5%, since GQ Lup is bright (more than 3000 counts inside a 2 pixel radius aperture). Table 1 shows the obtained apparent magnitudes and estimated error bars. Interstellar extinction, assuming $A_v = 0.4 \pm 0.2$ (Batalha et al. 2001) and the extinction law of Rieke & Lebofsky (1985), is also tabulated.

2.2. Subaru Photometry

Using the public Subaru archive (SMOKE), data for K, CH_4 and L$'$ filters were retrieved. For Kp and CH_4, since a dithered pattern was used to acquire GQ Lup A, a sky image was constructed from the median of all acquired images in each band. For L$'$, the sky image sequence was used to subtract the thermal background. Since no flat field images are available, images were simply registered at the image center, median combined, and a 180 degrees rotation was used to subtract the smooth PSF halo and residual sky background (an angle of 170 degrees was used for CH_4 data due to a bad pixel located at 180 degrees of GQ Lup Ab position). GQ Lup Ab is clearly visible in all three filters and was not saturated or occulted behind a coronagraph. Therefore, Δmag measurements were possible in each filter. GQ Lup Ab magnitude differences were found by optimizing the PSF subtraction from the PSF of GQ Lup A. Contrast measurements in L$'$ were corrected for an assumed 5% detector non-linearity, the level expected for the Aladin II array and measured GQ Lup A peak signal ($\sim$ 60,000 electrons). For CH_4 data, since the GQ Lup A peak signal approaches 100,000 electrons, a 5% non-linearity is assumed and a 0.1 mag is added to the magnitude error due to unmeasured detector non-linearity for that flux level. Magnitude errors were estimated by calculating the flux RMS variation of 10 square boxes of 1.5 λ/D width at 10 different angular positions and at the same separation as GQ Lup Ab. Apparent magnitudes were determined using known K, H and L$'$ magnitudes for GQ Lup A, H=7.70 ± 0.03 mag, K=7.10 ± 0.02 mag (2MASS) and L=6.05 ± 0.13 (Glass & Penston 1974; Hughes et al. 1994).

Magnitude differences between the L′ and the L filters are negligible. Our L′ magnitude differs by 0.8 magnitude compared to the one published by Neuhäuser et al. (2005) while the K (Ks for Neuhäuser et al. (2005)) magnitudes are consistent to 1 σ accuracy (see Table 1). A slice of the L′ image through GQ Lup A and Ab is given in Fig. 1; the Neuhäuser et al. (2005) measurement is likely contaminated by flux from the primary.

3. GQ Lup Ab Temperature and Radius Fit

A solar metalicity subset of the GAIA dusty model atmosphere grid (Hauschildt et al., in preparation) was used to fit the photometry in Sect. 2 and determine the radius and temperature of GQ Lup Ab. Given that surface gravity has only a small affect on predicted broad band photometry and that such young low-mass objects typically have low gravities, a standard $\log(g) = 3$ was assumed. The model fluxes were convolved and integrated over the appropriate transmission curves for each filter listed in Table 1. For the F814W HST filter, the total optical system transmission was used instead of the filter tranmission due a drop of sensitivity in a spectral region where GQ Lup Ab shows a significant increase of luminosity. These synthetic broad-band flux densities were interpolated to produce a uniform square grid in radius and temperature space. Observed magnitudes were corrected for distance and estimated interstellar reddening and transformed to fluxes using a calibrated Vega spectrum. The shape of the observed broad-band SED from R to L-band determines the effective temperature while the overall scaling needed to best match the observed fluxes (for a fix distance) determines the radius. A standard deviation for each model, $\sigma_{\rm model}$, was calculated using the following standard equation,

$$\sigma_{\rm model} = \sqrt{\frac{1}{N-1}\sum_{i=1}^{N}\left(\frac{o_i - m_i}{e_i}\right)^2}, \qquad (1)$$

where N is the number of photometric measurements and o, e and m are respectively the observe data point, its error bar, and expected model-derived flux. The F606W bandpass was not included since this point is clearly overluminous compared to the near-infrared bands (see Sect. 4). Figure 2 shows the temperature as a function of radius for GQ Lup Ab. Error contours are defined as models that deviate by 1, 3 and 5σ from the best fit model. The predicted temperature and radius of the Baraffe et al. (2003) evolution models for 1 and 5 Myrs and 7, 10, 12, 15 and 20 $M_{\rm Jup}$ are also shown. The best fit found is at 0.54σ from the model with an effective temperature of 2338K and radius of 0.37$R_{\odot}$ (assuming a distance of 140pc). The fit was then rerun for both maximum and minimum allowed distance and interstellar extinction to estimate error bars (see Table 2). The overall fit to account for both the distance and interstellar extinction is thus an effective temperature of 2338 ± 100K and a radius of range of $0.37 \pm 0.05 d_{140}$ $R_{\odot}$, where $d_{140} = d/140$ and d is the distance in parsecs. The resulting luminosity, accounting for the correlated error bars, is equal to $log(L/L_{\odot}) = -2.43 \pm 0.07 + log(d_{140}^2)$. Interstellar extinction does not significantly change the derived effective temperature but the distance adds a possible range three times the derived radius error bar. A better distance estimate would be required to further constrain the radius and the luminosity of GQ Lup Ab. At a 1σ confidence interval, our derived effective temperature has an error bar five times smaller than the one derived by Neuhäuser et al. (2005) and our radius is more than three times larger. Note that the radius ($0.12 \pm 0.06 R_{\odot}$), effective temperature (2050 ± 450) and luminosity ($log(L/L_{\odot}) = -2.37 \pm 0.41$) given in Neuhäuser et al. (2005); Neuhäuser (2005); Guenther et al. (2005) are incompatible; for such radius and temperature, the luminosity should be closer to $log(L/L_{\odot}) = -3.67$, clearly inconsistent with the observed photometry (see Fig. 3).

As discussed in Neuhäuser et al. (2005), planetary evolution models are highly uncertain for young objects. However, it is still interesting to compare our results to the Baraffe et al. (2003) evolution models, even if we know that they tend to underestimate the mass/overestimate luminosities (Mohanty et al. 2004; Reiners et al. 2005). At the nominal distance (140pc) and age (< 2 Myr). Our temperature and radius are consistent with a 13-20 $M_{\rm Jup}$ PMC/brown dwarf at 3σ. However, if the system is at 90pc or 190pc, GQ Lup Ab could respectively be a 9-16 $M_{\rm Jup}$ or a ~ 20 $M_{\rm Jup}$ companion (again at 3σ). Given the distance and age errors, we thus conclude that GQ Lup Ab can be a 9-20 $M_{\rm Jup}$ companion, or at the boundary between a PMC and brown dwarf similar to the Ab Pic PMC candidate (Chauvin et al. 2005b). Assuming a distance of 140pc and a slightly higher effective temperature of 2400K, our observations are consistent with a ~ 15 $M_{\rm Jup}$ brown dwarfs (Baraffe models) to 1σ accuracy. Observations better fit the evolution model if the system distance is less than 140pc.

It is clear from Fig. 3 that the F606W magnitude is overluminous compared to model predictions – the implications of this are discussed below. Including the F606W filter data point in the fit significantly reduce the quality of the fit (best fit of 6.6σ instead of 0.54σ).

4. Discussion

The HST F606W magnitude is significantly overluminous compared to model predictions (three magnitudes, see Fig 2). Such overluminosity can be explained by an unmodeled effect such as a bright Hα emission line from chromospheric activity, interaction with another undetected companion, flaring, accretion or some other unknown process. Assuming that the observed F606W overluminosity is coming from Hα emission, we can estimate the strength of emission by calculating the log ratio of its Hα luminosity to its bolometric luminosity. Using the simulated flux normalized spectrum for GQ Lup Ab, the F606W filter bandpass profile and assuming that all the observed flux in the F606W filter comes from a bright Hα emission line, we find GQ Lup Ab Hα emission strength $log(L_{H\alpha}/L_{\mathrm{bol}})$ of -1.71 ± 0.10, significantly larger, by an order of magnitude, than what is found for field M, L and T dwarfs (Gizis et al. 2000) or even in peculiar late type dwarfs (Liebert et al. 1999; Burgasser et al. 2000; Hall 2002; Burgasser et al. 2002). Such peculiar dwarfs are thought to be young low mass objects, ∼10 Myr 3-20 $\mathrm{M_{Jup}}$ (Liebert et al. 2003), though not as young as GQ Lup ; GQ Lup Ab could be a very young example, still bound with its primary, of such objects.

A visible spectrum of GQ Lup Ab is needed to confirm the Hα emission. If the Hα emission is present, the emission line 10% width can be used to discriminate between accretion and chromospheric activity (Muzerolle et al. 2003; Natta et al. 2004). Detection of Paβ and Brγ lines in the near-infrared could also be used to confirm accretion. Brγ was not detected in Neuhäuser et al. (2005); Guenther et al. (2005) K-band spectrum, but since this line is harder to detect and fainter than the Paβ line, such non-detection does not imply no ongoing accretion (Natta et al. 2004). A time series photometric/spectroscopic analysis could distinguish between transient emission due to a strong flare or constant emission characteristic of accretion. Searching for an eclipse could also confirm the interacting binary hypothesis. Strong Hα emission could also be a sign of a runaway accretion as postulated by Fortney et al. (2005) for the core accretion-gas capture model, although such observations would be very fortuitous due to the relatively short timescale expected for this phase. If GQ Lup Ab is strongly accreting, it may still be in its formation stage and its final mass would still be unknown.

5. Conclusion

We have reanalyzed available Subaru and HST data to fit GQ Lup Ab radius and effective temperature using model spectra. Our derived effective temperature (2338 ± 100K) is slightly hotter than the one derived by Neuhäuser et al. (2005) but with a substantially smaller error bar. Our derived radius for 140pc ($0.37 \pm 0.05\mathrm{R}_{\odot}$) is more than three times larger than what was found by Neuhäuser (2005). At that distance, our result is consistent to 1σ accuracy with a ∼15 $\mathrm{M_{Jup}}$ brown dwarfs (Baraffe models). If GQ Lup Ab is confirmed to be strongly accreting, it might be a young, still forming/contracting PMC or brown dwarf. A better distance estimate for the GQ Lup system is needed to further constrain its radius and luminosity. At the three sigma confidence interval, our measurement is consistent with a 9-20 M_{Jup} companion, at the mass boundary between PMC and brown dwarf.

Based in part on data collected at Subaru Telescope, which is operated by the NAO of Japan and also in part on observations made with the NASA/ESA HST, obtained from the data archive at the STScI. STScI is operated by the association of Universities for Research in Astronomy, Inc. under the NASA contract NAS 5-26555. This publication makes use of data products from 2MASS, which is a joint project of the University of Massachusetts and the IPAC/Caltech, funded by the NASA and NSF. This research was performed under the auspices of the DOE by the UC, LLNL under contract W-7405-ENG-48, and also supported in part by the NSF Science and Technology CFAO, managed by UCSC under cooperative agreement AST 98-76783. The authors thank Eric Becklin and Ben Zuckerman for helpful discussions.

REFERENCES

Baraffe, I., Chabrier, G., Barman, T. S., Allard, F., Hauschildt, P. H. 2003, A&A, 402, 701

Batalha, C., Lopes, D. F., Batalha, N. M. 2001, ApJ, 548, 377

Burgasser, A. J., Kirkpatrick, J. D., Reid, I. N., Liebert, J., Gizis, J. E., Brown, M. E. 2000, AJ, 120, 473

Burgasser, A. J., Liebert, J., Kirkpatrick, J. D., Gizis, J. E. 2002, AJ, 123, 2744

Chauvin, G., Lagrange, A.-M., Dumas, C., Zuckerman, B., Mouillet, D., Song, I., Beuzit, J.-L., Lowrance, P. 2005, A&A, 438, L25

Chauvin, G., Lagrange, A.-M., Zuckerman, B., Dumas, C., Mouillet, D., Song, I., Beuzit, J.-L., Lowrance, P., Bessell, M. S. 2005, A&A, 438, L29

Fortney, J. J., Marley, M. S., Hubickyj, O., Bodenheimer, P., Lissauer, J. J. 2005, Astronomische Nachrichten, 326, 925

Gizis, J. E., Monet, D. G., Reid, I. N., Kirkpatrick, J. D., Liebert, J., Williams, R. J. 2000, AJ, 120, 1085

Glass, I. S., Penston, M. V. 1974, MNRAS, 167, 237

Guenther, E. W., Neuhäuser, R., Wuchterl, G., Mugrauer, M., Bedalov, A., Hauschildt, P. H. 2005, proceeding of the workshop on Ultralow-mass star formation and evolution held in La Palama June 28 to July 1, 2005

Hall, P. B. 2002, ApJ, 564, L89

Hughes, J., Hartigan, P., Krautter, J., Kelemen, J. 1994, AJ, 108, 1071

Knude, J., Hog, E. 1998, A&A, 338, 897

Krist, J. 1993, Astronomical Data Analysis Software and Systems II, A.S.P. Conference Series, Vol. 52, 1993, R. J. Hanisch, R. J. V. Brissenden, and Jeannette Barnes, eds., 536

Liebert, J., Kirkpatrick, J. D., Reid, I. N., Fisher, M. D. 1999, ApJ, 519, 345

Liebert, J., Kirkpatrick, J. D., Cruz, K. L., Reid, I. N., Burgasser, A., Tinney, C. G., Gizis, J. E. 2003, AJ, 125, 343

Mohanty, S., Jayawardhana, R., Basri, G. 2004, ApJ, 609, 885

Murakawa, K. et al. 2004, PASJ, 56, 509

Muzerolle, J., Hillenbrand, L., Calvet, N., Briceño, C., Hartmann, L. 2003, ApJ, 592, 266

Natta, A., Testi, L., Muzerolle, J., Randich, S., Comerón, F., Persi, P. 2004, A&A, 424, 603

Neuhäuser, R., Brandner, W. 1998, A&A, 330, L29

Neuhäuser, R., Guenther, E. W., Wuchterl, G. Mugrauer, M., Bedalov, A., Hauschildt, P. H. 2005, A&A, 435, L13

Neuhäuser, R. 2005, ESO Workshop Proceedings on Multiple Stars, in press

Reiners, A., Basri, G., Mohanty, S. 2005, ApJ, 634, 1346

Rieke, G. H., Lebofsky, M. J. 1985, ApJ, 288, 618

Tachihara, K., Dobashi, K., Mizuno, A., Ogawa, H., Fukui, Y. 1996, PASJ, 48, 489

Wichmann, R., Bastian, U., Krautter, J., Jankovics, I., Rucinski, S. M. 1998, MNRAS, 301, L39

Whitmore, B., Heyer, I., Casertano, S. 1999, PASP, 111, 1559

Table 1: GQ Lup Ab Photometry

Filter	Vega Zpt	mag	mag (Neu05)	IE
F606W	22.92	19.19 ± 0.07	-	0.4 ± 0.2
F814W	21.67	17.67 ± 0.05	-	0.2 ± 0.1
CH_4off	-	13.76 ± 0.30	-	0.07 ± 0.04
F171M	20.19	13.84 ± 0.13	-	0.07 ± 0.04
F190N	18.48	14.08 ± 0.20	-	0.06 ± 0.03
F215N	18.25	13.40 ± 0.15	-	0.05 ± 0.02
K	-	13.37 ± 0.12	13.1 ± 0.1	0.05 ± 0.02
L'	-	12.52 ± 0.29	11.7 ± 0.3	0.02 ± 0.01

Table 2: Best Radius and Temperature Fit

	Dist. (pc)	IE_V	T_{eff}(K)	R ($R_\odot$)
	90	0.4	2338 ± 80	0.25 ± 0.03
Dist.	140	0.4	2338 ± 80	0.37 ± 0.05
	190	0.4	2338 ± 80	0.52 ± 0.07
	140	0.2	2320 ± 80	0.37 ± 0.05
IE	140	0.4	2338 ± 80	0.37 ± 0.05
	140	0.6	2360 ± 80	0.37 ± 0.05
Final	140	0.4	2338 ± 100	$0.37 \pm 0.05 d_{140}$

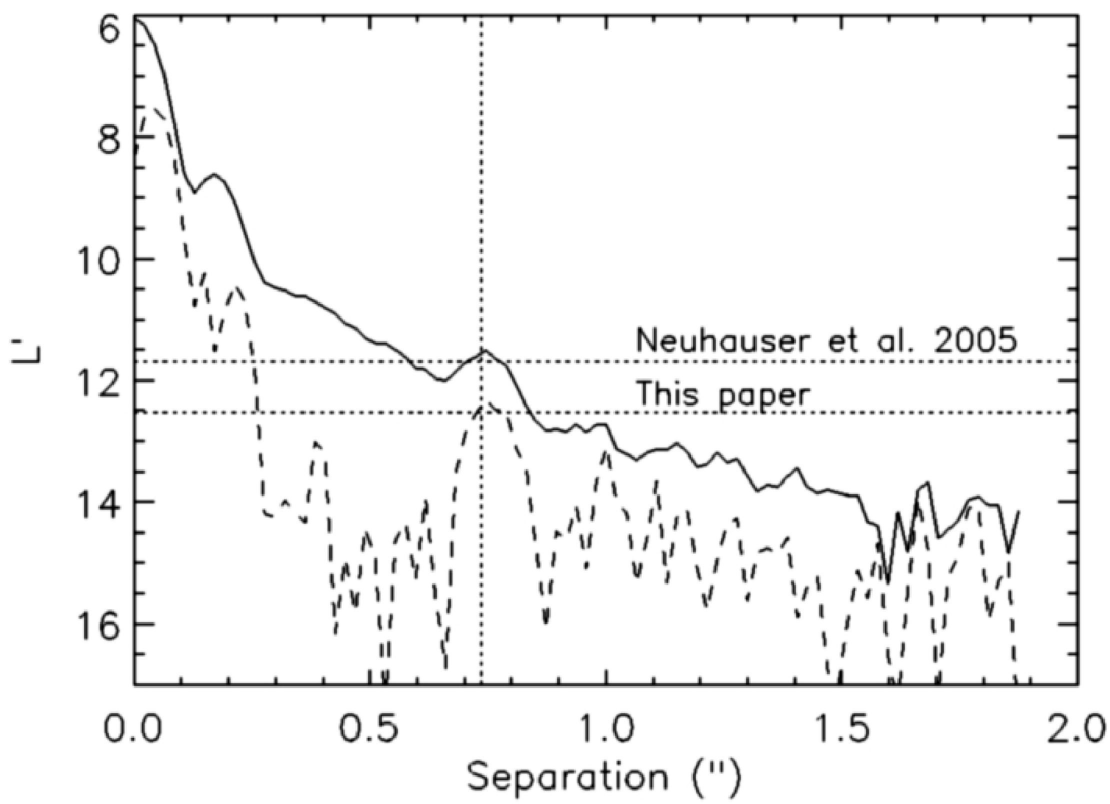

Fig. 1.— GQ Lup Ab L′ magnitude measurement. Solid line shows GQ Lup A PSF intensity profile going through GQ Lup Ab. Dotted vertical line shows the separation of GQ Lup Ab. Dashed line shows the same intensity profile after sky subtraction and GL Lup A PSF halo subtraction. The two horizonthal dotted lines show Neuhäuser et al. (2005) and our magnitude estimates.

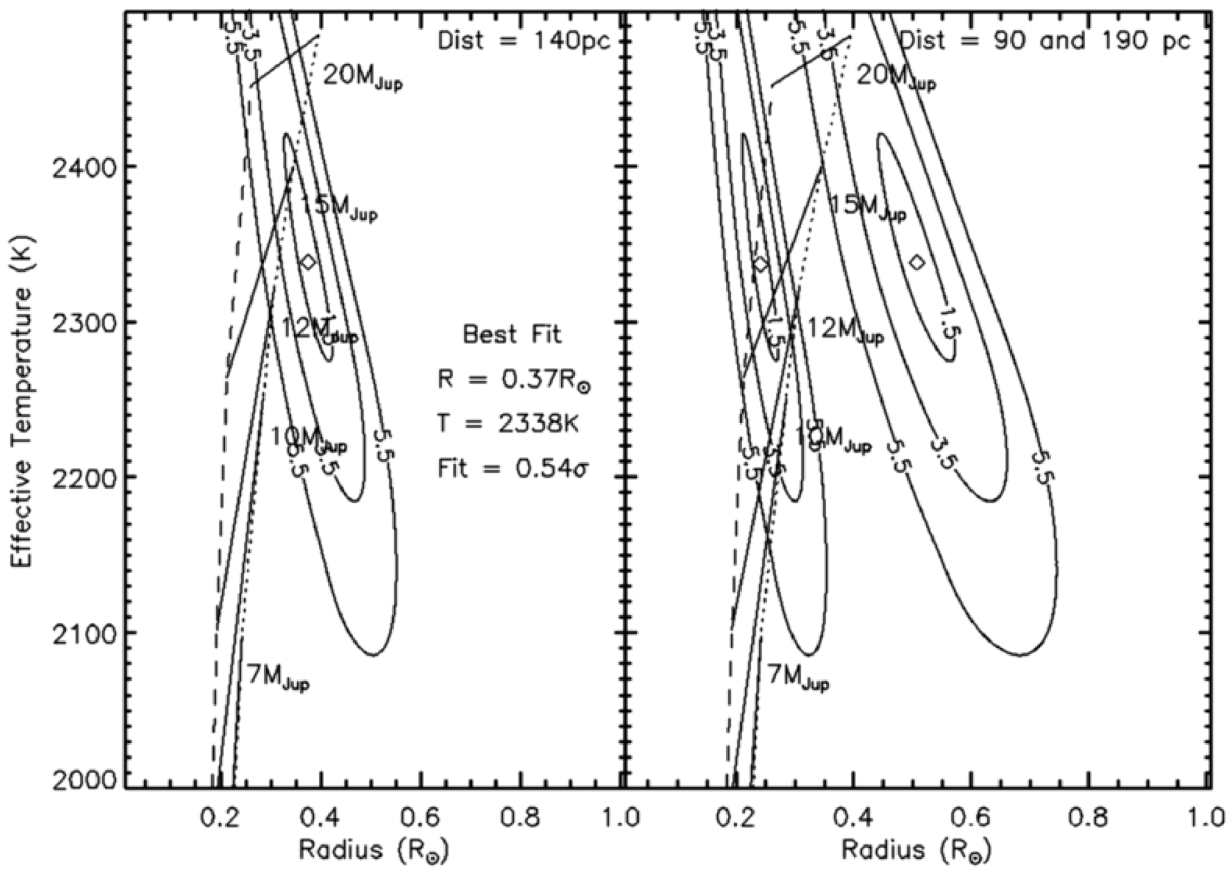

Fig. 2.— Temperature-radius fit for 140 (left) and 90 and 190pc (right) distance. The diamond symbol represents the best fit. Three contour levels at 1, 3 and 5σ from the best fit are shown. Model predictions for 7, 10, 12, 15 and 20 M_{Jup} and 1 (dotted line) and 5 Myr (dashed line) are also shown.

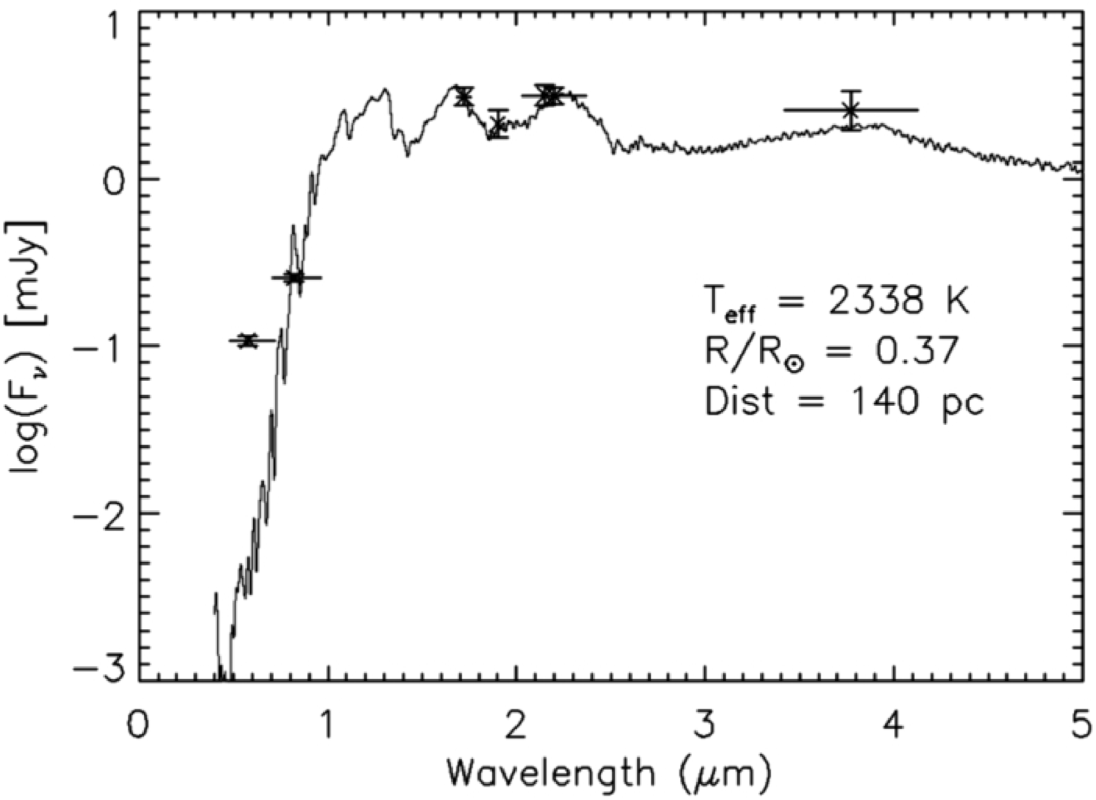

Fig. 3.— Best temperature-radius fit for 140pc, typical 0.4 IE in V band and 1 Myr. Luminosity is $log(L/L_{\odot}) = -2.43$.